

Influence of time-varying frequency content in earthquake ground motions on seismic response of linear elastic systems

Yong Li¹, Joel P. Conte^{1,*†} and Michele Barbato²

¹*Department of Structural Engineering, University of California at San Diego, La Jolla, CA 92093, USA*

²*Department of Civil and Environmental Engineering, Louisiana State University, Baton Rouge, LA 70803, USA*

SUMMARY

Earthquake ground motion records are nonstationary in both amplitude and frequency content. However, the latter nonstationarity is typically neglected mainly for the sake of mathematical simplicity. To study the stochastic effects of the time-varying frequency content of earthquake ground motions on the seismic response of structural systems, a pair of closely related stochastic ground motion models is adopted here. The first model (referred to as ground motion model I) corresponds to a fully nonstationary stochastic earthquake ground motion model previously developed by the authors. The second model (referred to as ground motion model II) is nonstationary in amplitude only and is derived from the first model. Ground motion models I and II have the same mean-square function and global frequency content but different features of time variation in the frequency content, in that no time variation of the frequency content exists in ground motion model II. New explicit closed-form solutions are derived for the response of linear elastic SDOF and MDOF systems subjected to stochastic ground motion model II. New analytical solutions for the evolutionary cross-correlation and cross-PSD functions between the ground motion input and the structural response are also derived for linear systems subjected to ground motion model I. Comparative analytical results are presented to quantify the effects of the time-varying frequency content of earthquake ground motions on the structural response of linear elastic systems. It is found that the time-varying frequency content in the seismic input can have significant effects on the stochastic properties of system response. Copyright © 2016 John Wiley & Sons, Ltd.

Received 20 May 2015; Revised 17 December 2015; Accepted 20 December 2015

KEY WORDS: stochastic earthquake ground motion model; nonstationarity; time-varying amplitude; time-varying frequency; linear elastic structural systems

1. INTRODUCTION

Data-driven analysis of recorded historical earthquake ground motions [1–6] and complex physics-based wave propagation theories [7] show that earthquake ground motion time histories are nonstationary in both amplitude and frequency content [8]. The time-varying intensity or nonstationarity in amplitude is typically characterized by the initial built-up phase, the high-intensity phase, and the gradually decaying tail. The time-varying frequency content or nonstationarity in frequency content can be attributed to the different arrival times at a given site of the P (primary or push), S (secondary or shear), and surface (Rayleigh and Love) waves, which propagate at different velocities through the earth crust and vary significantly in frequency content. Recorded earthquake accelerograms typically exhibit a temporal shift in frequency content toward lower frequencies [9]. Therefore, capturing the natural nonstationary characteristics of earthquake ground motions requires

*Correspondence to: Joel P. Conte, Department of Structural Engineering, University of California at San Diego, La Jolla, CA 92093, USA.

†E-mail: jpconte@ucsd.edu

a fully nonstationary stochastic ground motion model, which can be used to investigate the effects of the spectral nonstationarity of earthquake ground motions on structural response.

Stochastic ground motion models, which consider an actual ground motion record as a realization of an underlying random process, can be used to generate an arbitrary number of ground motion realizations (i.e., artificial ground motions). A number of stochastic earthquake ground motion models have been developed by ignoring the nonstationarity in frequency content, assuming that it has little effect on structural response [10]. In contrast, several fully nonstationary stochastic ground motion models were proposed accounting for the nonstationarity in both the amplitude and the frequency content. Their authors used them to show the influence of the frequency nonstationarity on linear elastic and nonlinear inelastic structural response, mainly of SDOF systems [11]. A nonstationary ground acceleration model with sectionally stationary frequency content (i.e., piecewise stationary in frequency content) was presented by Saragoni and Hart [11] and used to determine the significant effect of the time variation of the ground motion frequency content on the maximum relative displacement response of a stiffness degrading SDOF system. Using a modified version of the ground motion model proposed by Grigoriu *et al.* [12] with both amplitude and frequency modulation, Yeh and Wen [13] showed that the time-varying frequency content of ground excitation has significant effects on the response of inelastic deteriorating systems, especially when the dominant frequencies of ground excitation are close to the structural natural frequency. Beck and Papadimitriou [9] defined a new fully nonstationary stochastic ground motion model defined as the output of two cascaded SDOF linear elastic oscillators. The first oscillator has time-varying coefficients and is subjected to modulated white noise, while the second oscillator mimics Brune's source model [14] and provides the correct behavior of the spectral amplitudes at very low frequencies. The phenomenon referred to as moving resonance was demonstrated for the response of nonlinear elastic (softening) SDOF systems as well as the importance of modeling the temporal nonstationarity in the frequency content of ground motions. Moving resonance occurs when the lowering of the system frequencies, due to the decrease in stiffness with increasing response amplitude, tracks the shift of the dominant frequencies of the ground motion. Using a time-varying Autoregressive Moving Average (ARMA) earthquake model [15], Conte [16] investigated the effects of the frequency nonstationarity of earthquake ground motions on the response of nonlinear elastic and inelastic SDOF systems, which were found to be significant. Naga and Eatherton [17] used discrete wavelet transforms to analyze the spectral nonstationarity of earthquake ground acceleration time histories and corresponding SDOF system displacement response histories in order to investigate the moving resonance phenomenon for nonlinear elastic and inelastic SDOF systems. Wang *et al.* [18] proposed an approach for modeling and simulating nonstationary earthquake ground motions based on stationary wavelet and Hilbert transforms. The effects of the time-varying frequency content during the earthquakes were also examined using a joint time-frequency analysis technique of time signals to extract the nonstationary frequency information from the recorded data [19].

This paper employs a pair of closely related stochastic ground motion models ideally suited to investigate the effects of the time-varying frequency content of earthquake ground motions on structural response. A stochastic ground motion model previously developed [4], referred to as ground motion model I (GMM I) hereafter, is a fully nonstationary model (i.e., with time-varying amplitude and frequency content). A new ground motion model with nonstationarity in amplitude only, referred to as ground motion model II (GMM II) hereafter, is derived from GMM I by removing the nonstationarity in frequency content. These two ground motion models have the same mean-square ground acceleration function and the same average frequency content (i.e., frequency content averaged over the whole earthquake duration). GMM I can be calibrated (fitted) against any target (historical) ground motion record considered, and GMM II can be simply derived from the corresponding fitted GMM I.

This paper derives new closed-form random vibration solutions for the response of linear elastic (structural) systems subject to GMM II. New analytical solutions for the evolutionary cross-correlation and cross-power spectral density (PSD) functions between the seismic input and the structural response are also derived for linear systems subject to GMM I. These new closed-form solutions, together with existing closed-form solutions for GMM I [20], are used in this paper to demonstrate and investigate the effects of the nonstationarity in frequency content of earthquake ground motions on the response of linear elastic SDOF and MDOF systems.

2. EARTHQUAKE GROUND MOTION MODELS

Two closely related stochastic ground motion models are used in this paper to study the influence of the time-varying frequency content of earthquake ground motions on the response of structures. The first model (GMM I) was developed by Conte and Peng [4] from the family of sigma-oscillatory processes [21] and is fully nonstationary. To isolate the effect of the nonstationarity in frequency content in the comparison between the responses of structures to the two earthquake ground motion models, a second model (GMM II), which is nonstationary in amplitude only, is derived from GMM I such that the mean-square function and average frequency content (over the entire earthquake duration) of the ground acceleration process are the same for both ground motion models. The definition of GMM I is briefly reviewed later in the text as a basis to derive GMM II and for comparison between GMM I and GMM II.

2.1. Ground motion model I: nonstationary in both amplitude and frequency content

The stochastic GMM I is defined as the sum of a finite number of zero-mean, mutually independent, uniformly modulated Gaussian processes [4]. According to this model, the ground acceleration process, $\ddot{U}_g(t)$, is defined as

$$\ddot{U}_g(t) = \sum_{k=1}^p A_k(t) X_k(t) \quad (1)$$

where p is the number of process components or subprocesses, and $A_k(t)$ denotes the time modulating function of the k -th zero-mean stationary Gaussian component process $X_k(t)$, such that $A_k(t)X_k(t)$ is the k -th subprocess. The modulating function $A_k(t)$ is defined as

$$A_k(t) = \alpha_k (t - \zeta_k)^{\beta_k} e^{-\gamma_k(t - \zeta_k)} H(t - \zeta_k) \quad (2)$$

where α_k and γ_k are positive constants, β_k is a positive integer, and ζ_k denotes the ‘arrival time’ of the k -th subprocess; $H(t)$ is the unit step function. The k -th zero-mean Gaussian process, $X_k(t)$, is characterized by its autocorrelation function (ACF) and PSD function, which are given by Eqs. (3) and (4), respectively, as

$$R_{X_k X_k}(\tau) = e^{-v_k |\tau|} \cos(\eta_k \tau) \quad (3)$$

$$\Phi_{X_k X_k}(\omega) = \frac{v_k}{2\pi} \left[\frac{1}{(v_k)^2 + (\omega + \eta_k)^2} + \frac{1}{(v_k)^2 + (\omega - \eta_k)^2} \right] \quad (4)$$

in which v_k and η_k are two free parameters representing the frequency bandwidth and predominant (or central) frequency of the process $X_k(t)$, respectively. The mean-square function and evolutionary (time dependent) PSD (EPSD) function of GMM I [4] are given by

$$E \left[|\ddot{U}_g(t)|^2 \right] = \int_{-\infty}^{+\infty} \sum_{k=1}^p |A_k(t)|^2 \Phi_{X_k X_k}(\omega) d\omega = \sum_{k=1}^p |A_k(t)|^2 \quad (5)$$

$$\Phi_{\ddot{U}_g \ddot{U}_g}(\omega, t) = \sum_{k=1}^p |A_k(t)|^2 \Phi_{X_k X_k}(\omega) \quad (6)$$

respectively, where the property $\int_{-\infty}^{+\infty} \Phi_{X_k X_k}(\omega) d\omega = R_{X_k X_k}(\tau = 0) = 1.0$ is used to derive Eq. (5). The parameters of the stochastic GMM I in Eq. (1) are estimated such that the analytical EPSD function, $\Phi_{\ddot{U}_g \ddot{U}_g}(\omega, t)$ in Eq. (6), best fits, in the least-square sense, the EPSD function of the target earthquake accelerogram estimated using the short-time Thomson’s multiple-window method [4].

2.2. Ground motion model II: nonstationary in amplitude only

The new stochastic GMM II is derived from GMM I as a special case of sigma-oscillatory process and can be expressed in the same form as Eq. (1), that is,

$$\tilde{U}_g(t) = \sum_{k=1}^p A_k(t) \tilde{X}_k(t) \tag{7}$$

where the superimposed ‘~’ denotes GMM II. All component processes $\tilde{X}_k(t)$ have the same PSD function defined as the globally time-averaged PSD function of GMM I, that is,

$$\Phi_{\tilde{X}_k \tilde{X}_k}(\omega) = \Phi_{avg}(\omega) = \frac{\int_0^{t_d} \Phi_{\tilde{U}_g \tilde{U}_g}(\omega, t) dt}{\int_0^{t_d} \int_{-\infty}^{+\infty} \Phi_{\tilde{U}_g \tilde{U}_g}(\omega, t) d\omega dt} = \frac{\sum_{m=1}^p \rho_m \Phi_{X_m X_m}(\omega)}{\sum_{n=1}^p \rho_n} \tag{8}$$

where t_d denotes the duration of the earthquake ground motion record considered and ρ_k is the participation coefficient of the k -th subprocess of GMM I and is explicitly computed as

$$\rho_k = \int_0^{t_d} |A_k(t)|^2 dt = \frac{(2\beta_k)!}{(2\gamma_k)^{2\beta_k+1}} \alpha_k^2 + \alpha_k^2 e^{-2\gamma_k(t_d - \zeta_k)} \sum_{r=0}^{2\beta_k} (-1)^r \frac{(2\beta_k)!}{(2\beta_k - r)!} \frac{(t_d - \zeta_k)^{2\beta_k - r}}{(-2\gamma_k)^{r+1}} \tag{9}$$

The EPSD function of GMM II is given by

$$\Phi_{\tilde{U}_g \tilde{U}_g}(\omega, t) = \sum_{k=1}^p \left\{ |A_k(t)|^2 \Phi_{\tilde{X}_k \tilde{X}_k}(\omega) \right\} = \sum_{k=1}^p \left\{ |A_k(t)|^2 \tilde{\Phi}_{avg}(\omega) \right\} = \tilde{\Phi}_{avg}(\omega) \sum_{k=1}^p \left\{ |A_k(t)|^2 \right\} \tag{10}$$

Equation (10) indicates that GMM II is a uniformly modulated process and therefore nonstationary in amplitude only. It should be noted that the globally time-averaged PSD function of GMM II is identical to that of GMM I, that is,

$$\tilde{\Phi}_{avg}(\omega) = \frac{\int_0^{t_d} \Phi_{\tilde{U}_g \tilde{U}_g}(\omega, t) dt}{\int_0^{t_d} \int_{-\infty}^{+\infty} \Phi_{\tilde{U}_g \tilde{U}_g}(\omega, t) d\omega dt} = \frac{\sum_{k=1}^p \rho_k \tilde{\Phi}_{avg}(\omega)}{\sum_{n=1}^p \rho_n} = \Phi_{avg}(\omega) \tag{11}$$

The mean-square function of GMM II is identical to that of GMM I (Eq. (5)), that is,

$$E \left[\left| \tilde{U}_g(t) \right|^2 \right] = \int_{-\infty}^{+\infty} \sum_{k=1}^p |A_k(t)|^2 \tilde{\Phi}_{avg}(\omega) d\omega = \sum_{k=1}^p |A_k(t)|^2 \tag{12}$$

The previous analytical formulation of GMM I and GMM II can be used for analytical random vibration analysis of the effects of the nonstationarity in frequency content of earthquake ground motions on the response of linear elastic structures, which is the subject of the remainder of this paper. It can also be used to simulate ensembles of artificial earthquake ground acceleration records and investigate the effects of the time-varying frequency content of earthquake ground motions on the response of nonlinear elastic and inelastic structures. The parameters of GMM I (i.e., six parameters for each subprocess) must be calibrated based on a target historical earthquake record [4] or a target evolutionary PSD function. Because GMM II is derived directly from GMM I, only the same parameters of GMM I are needed for its complete definition.

3. CALIBRATION OF STOCHASTIC GROUND MOTION MODEL

The fully nonstationary earthquake GMM I is calibrated to the following two historical earthquake records: (i) the S00E (N-S) component of the May 18, 1940 Imperial Valley earthquake recorded at the El Centro Station, referred to as El Centro 1940; and (ii) the N90W (W-E) component of the October 17, 1989 Loma Prieta earthquake recorded at the Capitola station, referred to as Capitola 1989. Additional results for the N00W (N-S) component of the February 9, 1971 San Fernando earthquake recorded at the Orion Blvd. station can be found in the study of Li *et al.* [22] and are not reported here because of space limitations.

Figures 1 and 2 plot the EPSD functions of GMM I and GMM II for the two earthquake records defined previously. As expected, the ground motion frequency content (i.e., the shape of the ‘instantaneous’ PSD) varies with time for GMM I, while it remains time invariant for GMM II. In fact, all component processes of GMM II introduced in Eq. (7) have the same PSD function, as defined by Eq. (8), whereas the component processes of GMM I introduced in Eq. (1) have different PSD functions, as defined by Eq. (4). As illustration, single realizations of ground acceleration time histories generated from GMM I and GMM II are plotted in Figure 3(b) and 3(c), respectively, and compared with the target earthquake record, namely Capitola 1989, shown in Figure 3(a). It can be observed that both the target record and the realization from GMM I are nonstationary in frequency content (i.e., have a time-varying frequency content), while the realization from GMM II has a time-invariant frequency content. All three ground acceleration time histories are nonstationary in amplitude.

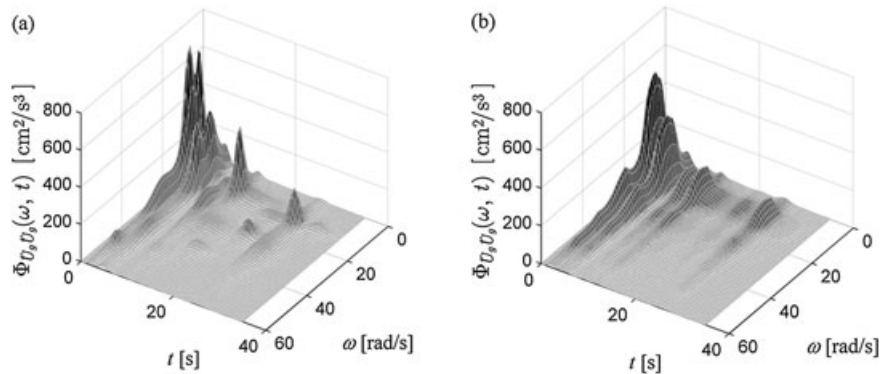


Figure 1. EPSD of ground motion model for El Centro 1940: (a) GMM I and (b) GMM II.

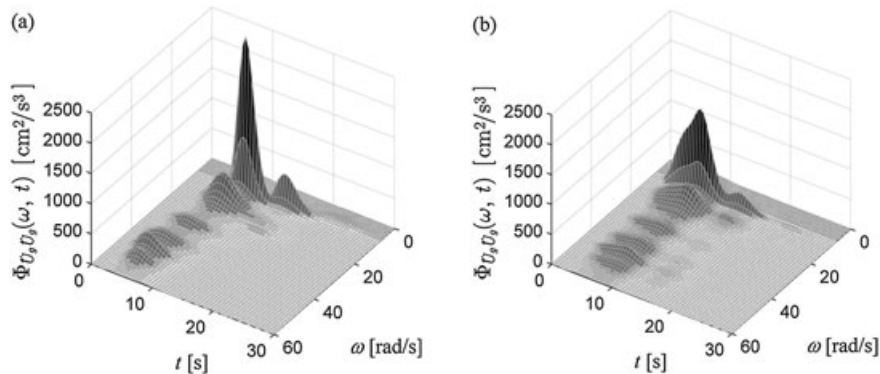


Figure 2. EPSD of ground motion model for Capitola 1989: (a) GMM I and (b) GMM II.

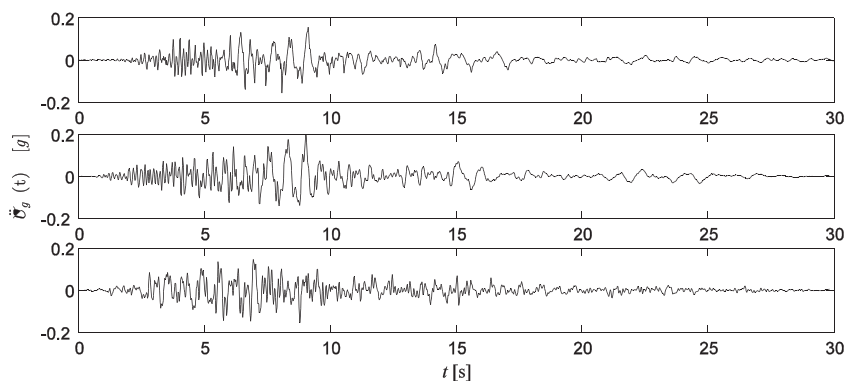


Figure 3. (a) Target earthquake record (Capitola 1989), (b) artificial realization from GMM I, and (c) artificial realization from GMM II.

4. STOCHASTIC RESPONSE OF LINEAR MDOF SYSTEMS

Peng and Conte [20] derived closed-form solutions for the evolutionary correlation and PSD matrices characterizing the nonstationary response of linear elastic classically and nonclassically damped MDOF systems subject to the fully nonstationary stochastic GMM I. This section presents new closed-form solutions for the response of linear elastic MDOF systems to stochastic GMM II as well as for the evolutionary cross-correlation and cross-PSD functions between the ground motion input and the system response to GMM I and GMM II.

4.1. Equations of motion and complex modal decomposition

The equations of motion of a linear elastic MDOF system with n degrees of freedom subjected to uniform (i.e., rigid base) excitation can be expressed in matrix form [23] as

$$\mathbf{M}\ddot{\mathbf{U}}(t) + \mathbf{C}\dot{\mathbf{U}}(t) + \mathbf{K}\mathbf{U}(t) = -\mathbf{M}\mathbf{L}\mathbf{F}(t) \quad (13)$$

where \mathbf{M} , \mathbf{C} , and \mathbf{K} are the mass, damping, and stiffness matrices, respectively, of dimension $(n \times n)$; $\mathbf{U}(t)$, $\dot{\mathbf{U}}(t)$, and $\ddot{\mathbf{U}}(t)$ are the vectors of nodal displacements, velocities, and accelerations with respect to the ground, respectively, of dimension $(n \times 1)$; \mathbf{L} is the influence coefficient matrix of dimension $(n \times p)$; and $\mathbf{F}(t)$ is the vector of (1 to 6) ground motion components of dimension $(p \times 1)$, which, in the case of a single-component (horizontal) random seismic excitation, as assumed in this paper, is a scalar loading function $F(t) = \ddot{u}_g(t)$ modeled as a random process. Equation (13) can be recast in state-space form as

$$\dot{\mathbf{Z}}(t) = \mathbf{G}\mathbf{Z} + \bar{\mathbf{P}}\mathbf{F}(t) \quad (14)$$

where $\mathbf{Z}(t) = \begin{pmatrix} \mathbf{U}(t) \\ \dot{\mathbf{U}}(t) \end{pmatrix}_{2n \times 1}$ is the state vector, $\mathbf{G} = \begin{pmatrix} \mathbf{0}_{n \times n} & \mathbf{I}_{n \times n} \\ -\mathbf{M}^{-1}\mathbf{K} & -\mathbf{M}^{-1}\mathbf{C} \end{pmatrix}_{2n \times 2n}$ is the system matrix, and $\bar{\mathbf{P}} = \begin{pmatrix} \mathbf{0}_{n \times 1} \\ -\mathbf{L} \end{pmatrix}_{2n \times 1}$ is the input matrix; bold characters identify vector/matrix quantities, and the subscripts indicate the dimensions of matrices and vectors. Using the complex modal matrix \mathbf{T} formed from the complex eigenmodes of matrix \mathbf{G} , the first-order state-space equation of motion (Eq. (14)) can be uncoupled into $2n$ first-order differential equations for the normalized complex modal coordinates $S_i(t)$ ($i = 1, \dots, 2n$):

$$\dot{S}_i(t) = \lambda_i S_i(t) + F(t), \quad i = 1, \dots, 2n \quad (15)$$

in which λ_i ($i=1, \dots, 2n$) are the $2n$ complex eigenvalues (complex conjugate by pairs) of the system matrix \mathbf{G} . Assuming that the system is initially at rest, the solution of Eq. (15) for the normalized complex modal response, $S_i(t)$, can be expressed as

$$S_i(t) = \int_0^t e^{\lambda_i(t-\tau)} F(\tau) d\tau, \quad i = 1, \dots, 2n \quad (16)$$

4.2. Stochastic ground motion model I

Using Priestley's evolutionary spectral theory [21], the k -th component or subprocess of the stochastic ground motion process $F(t) = \dot{U}_g(t)$ (Eq. (1)) can be expressed in Fourier–Stieltjes integral form as

$$\dot{U}_g^{[k]}(t) = \int_{-\infty}^{+\infty} A_k(t) e^{j\omega t} dZ_k(\omega) \quad (17)$$

where $j = \sqrt{-1}$ and $dZ_k(\omega)$ is the zero-mean orthogonal-increment process with the property

$$E[dZ_k^*(\omega_1) dZ_k(\omega_2)] = \Phi_{X_k X_k}(\omega_1) \delta(\omega_1 - \omega_2) d\omega_1 d\omega_2 \quad (18)$$

Substituting the k -th component process $\dot{U}_g^{[k]}(t)$ of the ground motion input given by Eq. (17) into the expression for the normalized complex modal response given by Eq. (16) yields

$$S_i^{[k]}(t) = \int_0^t e^{\lambda_i(t-\tau)} \int_{-\infty}^{+\infty} A_k(\tau) e^{j\omega\tau} dZ_k(\omega) d\tau = \int_{-\infty}^{+\infty} m_i^{[k]}(\omega, t) e^{j\omega t} dZ_k(\omega) \quad (19)$$

where $m_i^{[k]}(\omega, t)$ is the time-frequency modulating function of the i -th normalized complex modal response to the k -th subprocess of the ground motion input. By substituting the expression for $A_k(t)$ given by Eq. (2) into Eq. (19), the following expression for $m_i^{[k]}(\omega, t)$, which is the same for GMM I and GMM II, is obtained [20] as

$$m_i^{[k]}(\omega, t) = \alpha_k (\beta_k!) \left[e^{-\gamma_k t} \left(\sum_{n=0}^{\beta_k} \frac{(-1)^n t^{(\beta_k-n)}}{(\beta_k-n)! (j\omega - \lambda_i - \gamma_k)^{n+1}} \right) - \frac{(-1)^{\beta_k} e^{(\lambda_i - j\omega)t}}{\alpha^{(\beta_k+1)}} \right] \quad (20)$$

The auto/cross-correlation function of the normalized complex modal responses $S_i^{[k]}(t)$ and $S_j^{[k]}(t)$ to the k -th subprocess of the ground motion input $\dot{U}_g(t)$ is obtained as

$$R_{S_i^{[k]} S_j^{[k]}}(t, \tau) = E[S_i^{[k]*}(t) S_j^{[k]}(t + \tau)] = \int_{-\infty}^{+\infty} [m_i^{[k]}(\omega, t)]^* \Phi_{X_k X_k}(\omega) m_j^{[k]}(\omega, t + \tau) e^{j\omega\tau} d\omega \quad (21)$$

where τ denotes the time lag. A closed-form solution for $R_{S_i^{[k]} S_j^{[k]}}(t, \tau)$ is given by Peng and Conte [20].

The evolutionary auto/cross-PSD function of $S_i^{[k]}(t)$ and $S_j^{[k]}(t)$ is given by

$$\Phi_{S_i^{[k]} S_j^{[k]}}(\omega, t) = [m_i^{[k]}(\omega, t)]^* \Phi_{X_k X_k}(\omega) [m_j^{[k]}(\omega, t)] \quad (22)$$

In addition to the closed-form solutions for the evolutionary correlation and PSD matrices of the nonstationary response of linear elastic MDOF systems to GMM I developed by Peng and Conte [20] and recalled previously, newly derived closed-form solutions for the cross-correlation and cross-PSD functions between the earthquake input and the structural response are presented next.

The cross-correlation between the k -th subprocess of the ground motion input, $\dot{U}_g^{[k]}(t)$, and the j -th normalized complex modal response, $S_j^{[k]}(t)$, is given by

$$\mathbf{R}_{\ddot{U}_g S_j^{[k]}}(t, \tau) = E \left[\ddot{U}_g^{[k]*}(t) S_j^{[k]}(t + \tau) \right] = \int_{-\infty}^{+\infty} A_k(t) \Phi_{X_k X_k}(\omega) m_j^{[k]}(\omega, t + \tau) e^{j\omega\tau} d\omega \quad (23)$$

After extensive algebraic manipulations [22], the previous integral can be solved explicitly as

$$\begin{aligned} \mathbf{R}_{\ddot{U}_g S_j^{[k]}}(t, \tau) &= A_k(t) \int_0^{t+\tau} e^{\lambda_j(t+\tau-s)} A_k(s) \left[\int_{-\infty}^{+\infty} e^{j\omega(s-t)} \Phi_{X_k X_k}(\omega) d\omega \right] ds \\ &= (\alpha_k)^2 (t')^{\beta_k} e^{\lambda_j(t+\tau) - \gamma_k t'} \left[\begin{aligned} &\left(D_1 e^{-v_k t'} + D_3 e^{v_k t'} \right) \cos(bt') + \\ &\left(D_2 e^{-v_k t'} + D_4 e^{v_k t'} \right) \sin(bt') \end{aligned} \right], \text{ for } t' \geq 0 \quad (24) \end{aligned}$$

in which $t' = t - \zeta_k$ is the time elapsed from the start of the k -th subprocess of the ground motion input, $\ddot{U}_g^{[k]}(t)$, and the constants D_1 to D_4 are given by

$$\begin{aligned} D_1 &= e^{a_1 t'} \left(\sum_{m=0}^{\beta_k} \frac{(-1)^m (\beta_k!) (t')^{\beta_k - m}}{(\beta_k - m)! \left(\sqrt{a_1^2 + b^2} \right)^{m+1}} [\sin(bt') C_1(m+1) - \cos(bt') S_1(m+1)] \right) \\ &\quad + \frac{(-1)^{\beta_k} (\beta_k!)}{\left(\sqrt{a_1^2 + b^2} \right)^{\beta_k + 1}} S_1(\beta_k + 1) \\ D_2 &= e^{a_1 t'} \left(\sum_{m=0}^{\beta_k} \frac{(-1)^m (\beta_k!) (t')^{\beta_k - m}}{(\beta_k - m)! \left(\sqrt{a_1^2 + b^2} \right)^{m+1}} [\cos(bt') C_1(m+1) + \sin(bt') S_1(m+1)] \right) \\ &\quad - \frac{(-1)^{\beta_k} (\beta_k!)}{\left(\sqrt{a_1^2 + b^2} \right)^{\beta_k + 1}} C_1(\beta_k + 1) \\ D_3 &= e^{a_4(t'+\tau)} \left(\sum_{m=0}^{\beta_k} \frac{(-1)^m (\beta_k!) (t'+\tau)^{\beta_k - m}}{(\beta_k - m)! \left(\sqrt{a_4^2 + b^2} \right)^{m+1}} [\sin(b(t'+\tau)) C_4(m+1) - \cos(b(t'+\tau)) S_4(m+1)] \right) \\ &\quad - e^{a_4 t'} \left(\sum_{m=0}^{\beta_k} \frac{(-1)^m (\beta_k!) (t')^{\beta_k - m}}{(\beta_k - m)! \left(\sqrt{a_4^2 + b^2} \right)^{m+1}} [\sin(bt') C_4(m+1) - \cos(bt') S_4(m+1)] \right) \\ D_4 &= e^{a_4(t'+\tau)} \left(\sum_{m=0}^{\beta_k} \frac{(-1)^m (\beta_k!) (t'+\tau)^{\beta_k - m}}{(\beta_k - m)! \left(\sqrt{a_4^2 + b^2} \right)^{m+1}} [\cos(b(t'+\tau)) C_4(m+1) + \sin(b(t'+\tau)) S_4(m+1)] \right) \\ &\quad - e^{a_4 t'} \left(\sum_{m=0}^{\beta_k} \frac{(-1)^m (\beta_k!) (t')^{\beta_k - m}}{(\beta_k - m)! \left(\sqrt{a_4^2 + b^2} \right)^{m+1}} [\cos(bt') C_4(m+1) + \sin(bt') S_4(m+1)] \right) \end{aligned}$$

where

$$a_1 = -(\lambda_j - \nu_k + \gamma_k), \quad a_4 = -(\lambda_j + \nu_k + \gamma_k), \quad b = \eta_k$$

$$S_i(1) = b/\sqrt{a_i^2 + b^2}, \quad C_i(1) = a_i/\sqrt{a_i^2 + b^2}, \quad i = 1, 4$$

$$\begin{bmatrix} C_i(m+1) \\ S_i(m+1) \end{bmatrix} = \begin{bmatrix} C_i(1) & -S_i(1) \\ S_i(1) & C_i(1) \end{bmatrix} \begin{bmatrix} C_i(m) \\ S_i(m) \end{bmatrix}, \quad m = 1, \dots, \beta_k \text{ and } i = 1, 4$$

The evolutionary cross-PSD function between the k -th subprocess of the ground motion input, $\ddot{U}_g^{[k]}(t)$, and the j -th normalized complex modal response, $S_j^{[k]}(t)$, is given by

$$\Phi_{\ddot{U}_g^{[k]} S_j^{[k]}}(\omega, t) = A_k(t) \Phi_{X_k X_k}(\omega) [m_j^{[k]}(\omega, t)] \quad (25)$$

The component processes of the stochastic ground motion model defined in Eq. (1) are pairwise statistically independent. Therefore, the individual components of the evolutionary correlation and PSD matrices of the response of a linear elastic MDOF system, as well as the cross-correlation and cross-PSD functions between the ground motion input and the system response, can be obtained by summing the individual contributions of the component processes, that is,

$$\mathbf{R}_{S_i S_j}(t, \tau) = \sum_{k=1}^p \mathbf{R}_{S_i^{[k]} S_j^{[k]}}(t, \tau) \quad (26)$$

$$\Phi_{S_i S_j}(\omega, t) = \sum_{k=1}^p \Phi_{S_i^{[k]} S_j^{[k]}}(\omega, t) \quad (27)$$

$$\mathbf{R}_{\ddot{U}_g S_j}(t, \tau) = \sum_{k=1}^p \mathbf{R}_{\ddot{U}_g^{[k]} S_j^{[k]}}(t, \tau) \quad (28)$$

$$\Phi_{\ddot{U}_g S_j}(\omega, t) = \sum_{k=1}^p \Phi_{\ddot{U}_g^{[k]} S_j^{[k]}}(\omega, t) \quad (29)$$

After all entries of the evolutionary correlation and PSD matrices of the normalized complex modal response vector $\mathbf{S}(t) = [S_1(t) \ S_2(t) \ \dots \ S_{2n}(t)]^T$, namely $\mathbf{R}_{SS}(t, \tau)$ and $\Phi_{SS}(\omega, t)$, are obtained using Eqs. (26) and (27), the evolutionary correlation and PSD matrices, $\mathbf{R}_{ZZ}(t, \tau)$ and $\Phi_{ZZ}(\omega, t)$, of the state vector $\mathbf{Z}(t)$ are obtained using modal superposition as

$$\mathbf{R}_{ZZ}(t, \tau) = \bar{\mathbf{T}}^* \mathbf{R}_{SS}(t, \tau) \bar{\mathbf{T}}^T \quad (30)$$

$$\Phi_{ZZ}(\omega, t) = \bar{\mathbf{T}}^* \Phi_{SS}(\omega, t) \bar{\mathbf{T}}^T \quad (31)$$

where $\bar{\mathbf{T}}$ denotes the effective modal participation matrix defined as

$$\bar{\mathbf{T}} = \mathbf{T} \mathbf{\Gamma} \quad (32)$$

in which $\mathbf{\Gamma}$ is the diagonal modal participation factor matrix with diagonal terms defined as $\Gamma_i = (\mathbf{\Gamma})_{ii} = (\mathbf{T}^{-1}\mathbf{\bar{P}})_i$, $i = 1, \dots, 2n$.

Similarly, the evolutionary cross-correlation and cross-PSD matrices between the ground motion input $\ddot{U}_g(t)$ and the system state response $\mathbf{Z}(t)$ can be expressed as

$$\mathbf{R}_{\ddot{U}_g\mathbf{Z}}(t, \tau) = \mathbf{R}_{\ddot{U}_g\mathbf{S}}(t, \tau) \mathbf{\bar{T}}^T \quad (33)$$

$$\mathbf{\Phi}_{\ddot{U}_g\mathbf{Z}}(\omega, t) = \mathbf{\Phi}_{\ddot{U}_g\mathbf{S}}(\omega, t) \mathbf{\bar{T}}^T \quad (34)$$

4.3. Stochastic ground motion model II

This section focuses on the response of linear elastic MDOF systems subject to stochastic GMM II with amplitude nonstationarity and time-invariant frequency content. Similar to Eq. (17) for GMM I, the k -th component or subprocess of GMM II can be expressed in Fourier–Stieltjes integral form as

$$\tilde{U}_g^{[k]}(t) = \int_{-\infty}^{+\infty} A_k(t) e^{j\omega t} d\tilde{Z}_k(\omega) \quad (35)$$

where $d\tilde{Z}_k(\omega)$ is the zero-mean orthogonal-increment process characterized by

$$\mathbb{E} \left[d\tilde{Z}_k^*(\omega_1) d\tilde{Z}_k(\omega_2) \right] = \Phi_{\tilde{X}_k \tilde{X}_k}(\omega_1) \delta(\omega_1 - \omega_2) d\omega_1 d\omega_2 \quad (36)$$

Substituting the k -th component process $\tilde{U}_g^{[k]}(t)$ of the ground motion input in Eq. (35) into the expression for the normalized complex modal response in Eq. (16) gives

$$\tilde{S}_i^{[k]}(t) = \int_0^t e^{\lambda_i(t-\tau)} \int_{-\infty}^{+\infty} A_k(\tau) e^{j\omega\tau} d\tilde{Z}_k(\omega) d\tau = \int_{-\infty}^{+\infty} m_i^{[k]}(\omega, t) e^{j\omega t} d\tilde{Z}_k(\omega) \quad (37)$$

where $m_i^{[k]}(\omega, t)$ is defined in Eq. (20). Closed-form solutions for linear elastic MDOF systems subjected to GMM II, including evolutionary auto/cross-correlation and auto/cross-PSD functions of the system response as well as evolutionary cross-correlation and cross-PSD functions between ground motion input and system response, are derived in the remainder of this section, similar to the case of GMM I. The only difference with GMM I is that all p component processes of GMM II, $\tilde{U}_g^{[k]}(t)$ ($k = 1, \dots, p$), have the same PSD function, $\Phi_{\tilde{X}_k \tilde{X}_k}(\omega) = \tilde{\Phi}_{avg}(\omega)$ ($k = 1, \dots, p$), defined as the globally time-averaged PSD function of GMM I. Thus, the evolutionary auto/cross-PSD functions of the normalized complex modal responses $\tilde{S}_i^{[k]}(t)$ and $\tilde{S}_j^{[k]}(t)$ to the k -th subprocess of GMM II are obtained as

$$\Phi_{\tilde{S}_i^{[k]} \tilde{S}_j^{[k]}}(\omega, t) = [m_i^{[k]}(\omega, t)]^* \tilde{\Phi}_{avg}(\omega) [m_j^{[k]}(\omega, t)] \quad (38)$$

Correspondingly, the evolutionary auto/cross-correlation functions of the modal responses $\tilde{S}_i^{[k]}(t)$ and $\tilde{S}_j^{[k]}(t)$ to the k -th subprocess of GMM II, $A_k(t)\tilde{X}_k(t)$, are derived as

$$\begin{aligned} R_{\tilde{S}_i^{[k]} \tilde{S}_j^{[k]}}(t, \tau) &= E \left[\tilde{S}_i^{[k]*}(t) \tilde{S}_j^{[k]}(t + \tau) \right] = \int_{-\infty}^{+\infty} [m_i^{[k]}(\omega, t)]^* \Phi_{\tilde{X}_k \tilde{X}_k}(\omega) m_j^{[k]}(\omega, t + \tau) e^{j\omega\tau} d\omega \\ &= \sum_{m=1}^p \kappa_m R_{S_i^{[k,m]} S_j^{[k,m]}}(t, \tau) \end{aligned} \quad (39)$$

where

$$\kappa_m = \frac{\rho_m}{\sum_{n=1}^p \rho_n} \quad (40)$$

$$R_{S_i^{[k,m]} S_j^{[k,m]}}(t, \tau) = \int_{-\infty}^{+\infty} [m_i^{[k]}(\omega, t)]^* \Phi_{X_m X_m}(\omega) m_j^{[k]}(\omega, t + \tau) e^{j\omega\tau} d\omega \quad (41)$$

In Eq. (41), $R_{S_i^{[k,m]} S_j^{[k,m]}}(t, \tau)$ can be physically interpreted as the evolutionary cross-correlation function of the normalized complex modal responses $S_i^{[k,m]}(t)$ and $S_j^{[k,m]}(t)$ to a new subprocess defined by the m -th zero-mean stationary Gaussian process, $X_m(t)$, with PSD $\Phi_{X_m X_m}(\omega)$ defined in Eq. (4), modulated by the k -th time modulating function, $A_k(t)$, defined in Eq. (2); that is, $S_i^{[k,m]}(t)$ is the solution of Eq. (15) in which $F(t) = \dot{U}_g^{[k,m]} = A_k(t)X_m(t)$. The ‘crossing’ between the k -th modulating function $A_k(t)$ and the m -th zero-mean stationary Gaussian process $X_m(t)$ is due to the fact that, as expressed in Eq. (8), each stationary subprocess $\tilde{X}_k(t)$ ($k = 1, \dots, p$) of GMM II has a PSD function defined as a weighted average of the PSD functions of the stationary subprocesses $X_m(t)$ ($m = 1, \dots, p$) of GMM I. Comparison between Eqs. (41) and (21) indicates that $R_{S_i^{[k,m]} S_j^{[k,m]}}(t, \tau)$ can be computed in the same way as $R_{S_i^{[m]} S_j^{[m]}}(t, \tau)$ in Eq. (21) by substituting the parameters of the time modulating function $A_m(t)$ with those of $A_k(t)$.

The evolutionary cross-correlation function between the k -th subprocess of the ground motion input, $\tilde{U}_g^{[k]}(t)$ in GMM II, and the j -th normalized complex modal response, $\tilde{S}_j^{[k]}(t)$, is given by Eq. (42). Notice that the cross-correlation function $R_{\tilde{U}_g^{[k,m]} \tilde{S}_j^{[k,m]}}(t, \tau)$ in Eq. (42) can be derived using the solution for $R_{\tilde{U}_g^{[k]} \tilde{S}_j^{[k]}}(t, \tau)$ given by Eq. (24) by substituting the parameters of the PSD function $\Phi_{X_k X_k}(\omega)$ with those of the PSD function $\Phi_{X_m X_m}(\omega)$. The evolutionary cross-PSD function between the k -th subprocess of the ground motion input, $\tilde{U}_g^{[k]}(t)$, for GMM II, and the j -th normalized complex modal response, $\tilde{S}_j^{[k]}(t)$, is given by Eq. (43).

$$\begin{aligned} R_{\tilde{U}_g^{[k]} \tilde{S}_j^{[k]}}(t, \tau) &= E \left[\tilde{U}_g^{[k]*}(t) \tilde{S}_j^{[k]}(t + \tau) \right] = A_k(t) \int_0^{t+\tau} e^{j\omega(t+\tau-s)} A_k(s) \left[\int_{-\infty}^{+\infty} e^{j\omega(s-t)} \Phi_{\tilde{X}_k \tilde{X}_k}(\omega) d\omega \right] ds \\ &= \sum_{m=1}^p \left\{ \frac{\rho_m}{\sum_{n=1}^p \rho_n} A_k(t) \int_0^{t+\tau} e^{j\omega(t+\tau-s)} A_k(s) \left[\int_{-\infty}^{+\infty} e^{j\omega(s-t)} \Phi_{X_m X_m}(\omega) d\omega \right] ds \right\} \\ &= \sum_{m=1}^p \kappa_m R_{\tilde{U}_g^{[k,m]} \tilde{S}_j^{[k,m]}}(t, \tau) \end{aligned} \quad (42)$$

$$\Phi_{\tilde{U}_g^{[k]} \tilde{S}_j^{[k]}}(\omega, t) = A_k(t) \Phi_{\tilde{X}_k \tilde{X}_k}(\omega) [m_j^{[k]}(\omega, t)] \quad (43)$$

Taking advantage of the pairwise statistical independence of the component processes of stochastic GMM II, the evolutionary correlation and PSD matrices of the normalized complex modal responses to GMM II defined in Eq. (7) are obtained as

$$\mathbf{R}_{\tilde{S}_i \tilde{S}_j}(t, \tau) = \sum_{k=1}^p \mathbf{R}_{\tilde{S}_i^{[k]} \tilde{S}_j^{[k]}}(t, \tau) \quad (44)$$

$$\Phi_{\tilde{S}_i \tilde{S}_j}(\omega, t) = \sum_{k=1}^p \Phi_{\tilde{S}_i^{[k]} \tilde{S}_j^{[k]}}(\omega, t) \quad (45)$$

where $\mathbf{R}_{\tilde{S}_i^{[k]} \tilde{S}_j^{[k]}}(t, \tau)$ and $\Phi_{\tilde{S}_i^{[k]} \tilde{S}_j^{[k]}}(\omega, t)$ are given in Eqs. (39) and (38), respectively. Similarly, the evolutionary cross-correlation and cross-PSD functions between the ground motion input and the system modal responses are given by

$$\mathbf{R}_{\tilde{U}_g \tilde{S}_j}(t, \tau) = \sum_{k=1}^p \mathbf{R}_{\tilde{U}_g^{[k]} \tilde{S}_j^{[k]}}(t, \tau) \quad (46)$$

$$\Phi_{\tilde{U}_g \tilde{S}_j}(\omega, t) = \sum_{k=1}^p \Phi_{\tilde{U}_g^{[k]} \tilde{S}_j^{[k]}}(\omega, t) \quad (47)$$

After the evolutionary correlation and PSD matrices of the normalized complex modal response vector $\tilde{\mathbf{S}}(t) = [\tilde{S}_1(t) \ \tilde{S}_2(t) \ \dots \ \tilde{S}_{2n}(t)]^T$, $\mathbf{R}_{\tilde{\mathbf{S}}\tilde{\mathbf{S}}}(t, \tau)$ and $\Phi_{\tilde{\mathbf{S}}\tilde{\mathbf{S}}}(\omega, t)$, are obtained using Eqs. (44) and (45), the evolutionary correlation and PSD matrices of the state vector $\tilde{\mathbf{Z}}(t)$, $\mathbf{R}_{\tilde{\mathbf{Z}}\tilde{\mathbf{Z}}}(t, \tau)$ and $\Phi_{\tilde{\mathbf{Z}}\tilde{\mathbf{Z}}}(\omega, t)$, are obtained using modal superposition as

$$\mathbf{R}_{\tilde{\mathbf{Z}}\tilde{\mathbf{Z}}}(t, \tau) = \bar{\mathbf{T}}^* \mathbf{R}_{\tilde{\mathbf{S}}\tilde{\mathbf{S}}}(t, \tau) \bar{\mathbf{T}}^T \quad (48)$$

$$\Phi_{\tilde{\mathbf{Z}}\tilde{\mathbf{Z}}}(\omega, t) = \bar{\mathbf{T}}^* \Phi_{\tilde{\mathbf{S}}\tilde{\mathbf{S}}}(\omega, t) \bar{\mathbf{T}}^T \quad (49)$$

Similarly, the evolutionary cross-correlation and cross-PSD matrices between the ground motion input and the system state response $\tilde{\mathbf{Z}}(t)$ are obtained using modal superposition as

$$\mathbf{R}_{\tilde{U}_g \tilde{\mathbf{Z}}}(t, \tau) = \mathbf{R}_{\tilde{U}_g \tilde{\mathbf{S}}}(t, \tau) \bar{\mathbf{T}}^T \quad (50)$$

$$\Phi_{\tilde{U}_g \tilde{\mathbf{Z}}}(\omega, t) = \Phi_{\tilde{U}_g \tilde{\mathbf{S}}}(\omega, t) \bar{\mathbf{T}}^T \quad (51)$$

5. APPLICATION EXAMPLES

The closed-form solutions presented in Eqs. (30) to (34) for GMM I and Eqs. (48) to (51) for GMM II are applied in this section to SDOF and MDOF linear elastic systems. The visualization of the derived solutions is aimed to investigate analytically and systematically the effects of the time variation in the frequency content of earthquake ground motions on the response of linear elastic systems.

5.1. SDOF systems

This section presents the results for linear elastic SDOF systems with a damping ratio of 2% and natural periods of 0.5 and 1.5 s subjected to stochastic GMM I and GMM II. Similar results for more cases (i.e., different natural periods and damping ratios) can be found in [22]. Figures 4–7 show the EPSD, $\Phi_{UU}(\omega, t)$, of the relative displacement response, $U(t)$, of the linear elastic SDOF systems considered to the El Centro 1940 and Capitola 1989 stochastic ground motion models with (GMM I) and without (GMM II) time-varying frequency content. Additional results for the Orion Blvd. 1971 stochastic ground motion model can be found in the study of Li *et al.* [22]. The energy of the seismic response of these systems is narrowly concentrated at the natural frequency of the system in spite of the broadband seismic input (Figures 1 and 2). Furthermore, this energy's distribution over time differs significantly between GMM I and GMM II, especially for the SDOF

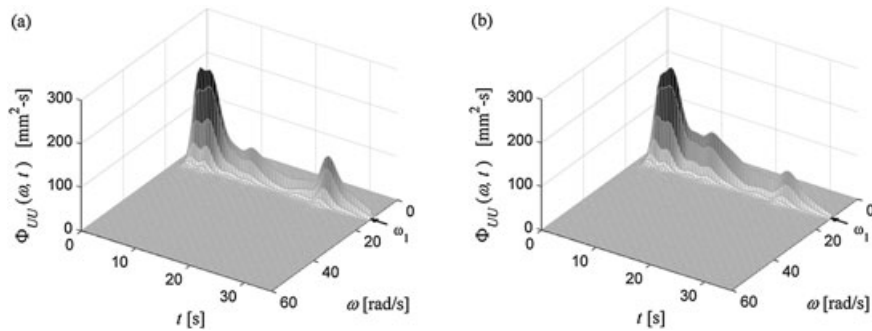


Figure 4. EPSD of U for linear elastic SDOF system with $T=0.5$ s under El Centro 1940: (a) GMM I and (b) GMM II.

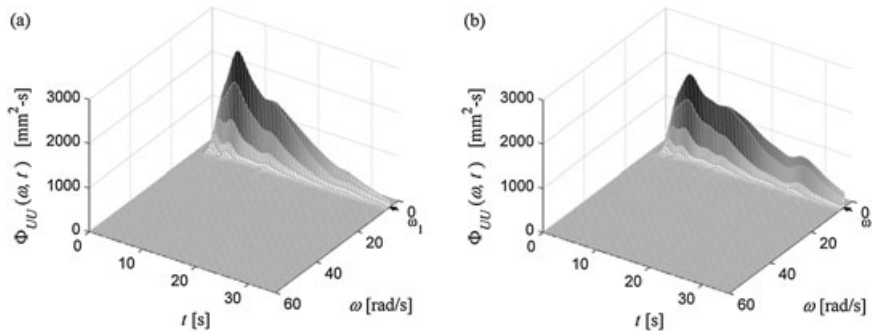


Figure 5. EPSD of U for linear elastic SDOF system with $T=1.5$ s under El Centro 1940: (a) GMM I and (b) GMM II.

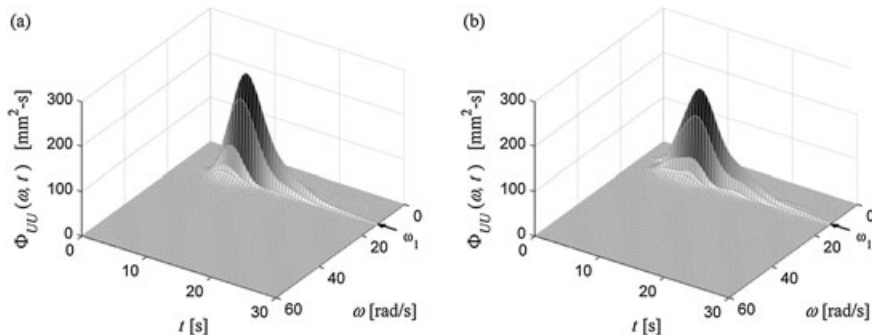


Figure 6. EPSD of U for linear elastic SDOF system with $T=0.5$ s under Capitola 1989: (a) GMM I and (b) GMM II.

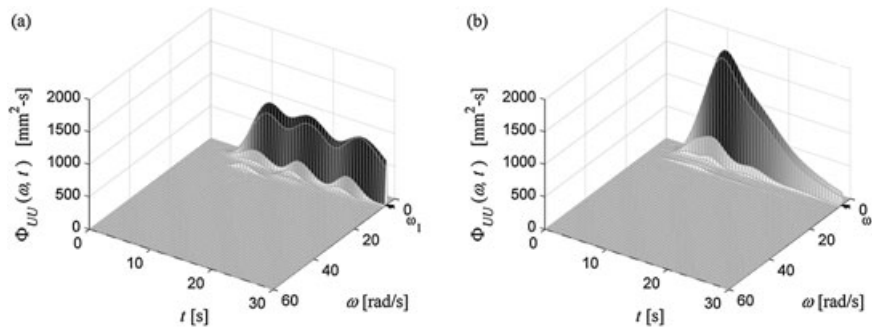


Figure 7. EPSD of U for linear elastic SDOF system with $T=1.5$ s under Capitola 1989: (a) GMM I and (b) GMM II.

with $T=1.5$ s. The same observation can also be made in Figures 8 and 9, which show the time histories of the root mean square (RMS) of $U(t)$, $RMS[U(t)] = \sqrt{E[U^2(t)]}$. In Figure 9(b), it is observed that the RMS relative displacement response of the linear elastic SDOF system with $T=1.5$ s is significantly higher for GMM I than for GMM II during the second half of the earthquake duration. This phenomenon is due to the fact that the frequency content of the ground motion around the natural frequency of the system is relatively higher for GMM I than for GMM II after $t=16$ s (see the low-frequency spectral peaks denoted as i, ii, and iii in Figure 10(a), which move toward the natural frequency of the system). It also explains the persistent strong amplitude vibration observed during the last 20 s of the earthquake duration for GMM I; see Figures 7(a) and 9(b). Relatively low amplitude components in the seismic input near the end of the earthquake (see

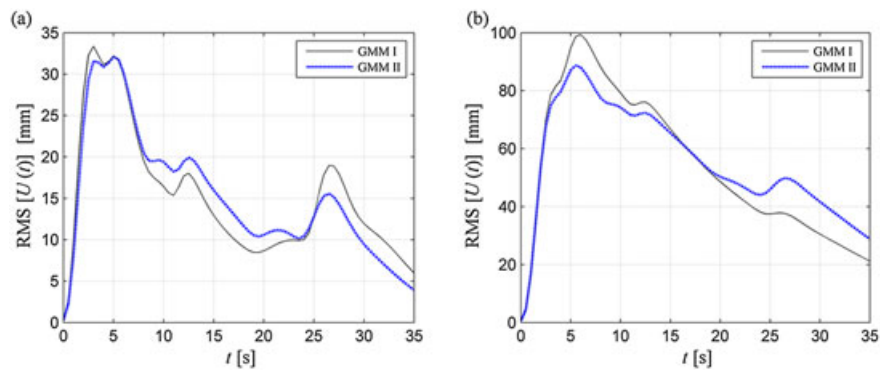


Figure 8. RMS of U for linear elastic SDOF system under El Centro 1940: (a) $T=0.5$ s and (b) $T=1.5$ s.

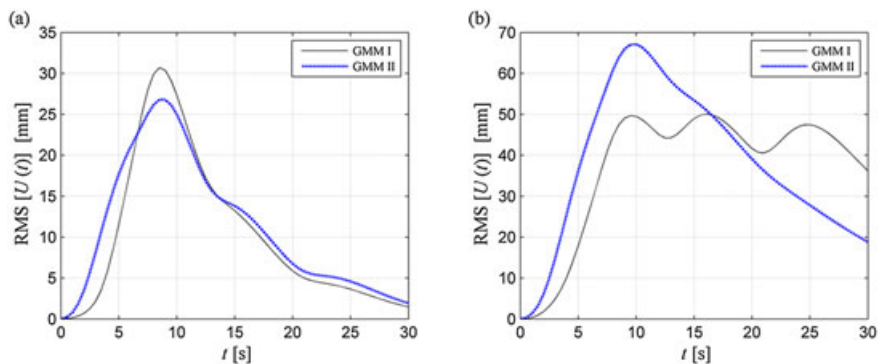


Figure 9. RMS of U for linear elastic SDOF system under Capitola 1989: (a) $T=0.5$ s and (b) $T=1.5$ s.

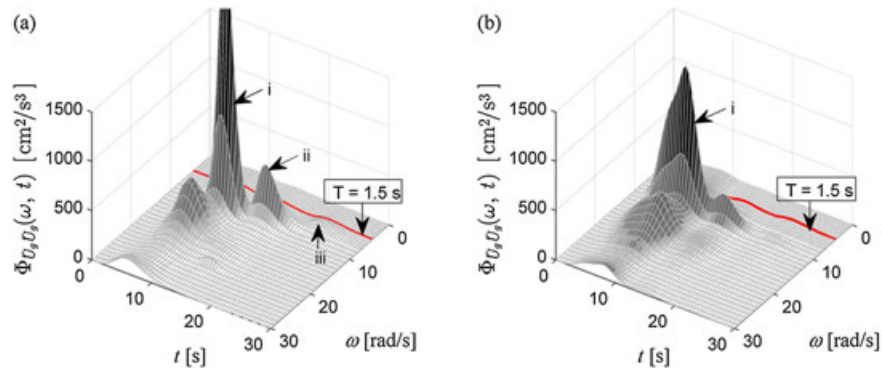


Figure 10. Close view of EPSP of ground motion model for Capitola 1989: (a) GMM I and (b) GMM II.

spectral peak iii in Figure 10(a) also produce a relatively large structural response, if the ground motion excitation frequency is close to the system frequency. This type of response feature can play a significant role, for example, for nonlinear systems with (effective) natural period(s) varying during the earthquake, which can be affected by the moving resonance phenomenon (i.e., the evolving, typically elongating, natural period(s) of the structure tune in with the varying frequency content of the earthquake ground motion). As shown in Figures 8 and 9, neglecting the frequency nonstationarity in earthquake ground motions may either increase or decrease significantly the peak RMS response and also may change notably the pattern of the RMS response history, depending on the period of the system and the spectrotemporal properties of the ground motion.

Figure 11 shows the evolutionary ACF, $R_{UU}(t, \tau)$, of the relative displacement response, $U(t)$, of the linear elastic SDOF system ($T=1.5$ s) to the Capitola 1989, which corresponds to the case with the largest difference between evolutionary ACFs for GMM I and GMM II. At $\tau=0$, the evolutionary ACF corresponds to the mean-squared response (i.e., the square of the RMS response plotted in Figure 9(b)), which has a different pattern for GMM I and GMM II (i.e., three peaks for GMM I versus a single peak for GMM II). This pattern is preserved along the time axis t of the 3D plot representation of $R_{UU}(t, \tau)$, which exhibits an oscillatory decay with a period of 1.5 s along the time lag axis τ because of damping effect.

5.2. MDOF systems

The second application example presented in this paper consists of the idealized three-dimensional, three-story, unsymmetrical building shown in Figure 12, which was taken from [12]. The three floors are modeled as rigid (inplane) diaphragms. The motion of each floor (# i) is represented by three DOFs defined at the center of mass (i.e., center of geometry) of the floor, namely the displacements relative to the ground in the X -direction, $U_{X_i}(t)$, and in the Y -direction, $U_{Y_i}(t)$, and the rotation relative to the ground about the vertical Z -axis, $\theta_{Z_i}(t)$. Table I reports the modal analysis

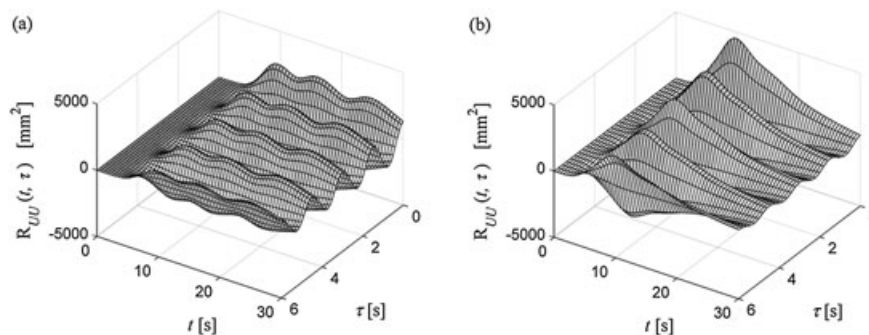


Figure 11. Evolutionary ACF of $U(t)$ for linear elastic SDOF system ($T=1.5$ s) under Capitola 1989: (a) GMM I and (b) GMM II.

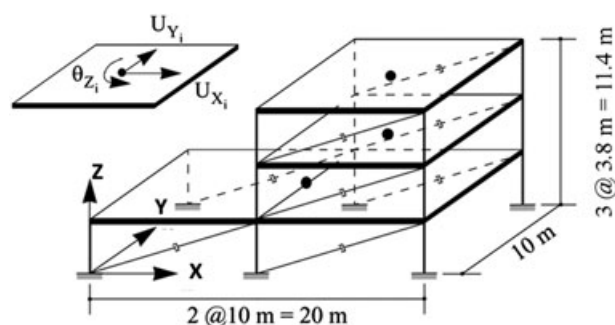


Figure 12. Three-dimensional, three-story, unsymmetrical building structure with rigid (inplane) diaphragms and three DOFs per floor.

Table I. Undamped natural frequencies and description of mode shapes of the 3D building.

Mode	Frequency [rad/s]	Mode shape description
1	16.0	Translation (X)
2	24.1	Lateral (Y)–torsional coupling
3	36.6	Translation (X)
4	41.2	Lateral (Y)–torsional coupling
5	56.7	Lateral (Y)–torsional coupling
6	57.0	Translation (X)
7	73.9	Lateral (Y)–torsional coupling
8	95.2	Lateral (Y)–torsional coupling
9	127.7	Lateral (Y)–torsional coupling

results (natural frequencies and mode shape description) for the undamped condition. Both classical damping with 2% damping ratio per mode and nonclassical damping (realized by the diagonal viscous dampers shown in Figure 12 in addition to the classical damping case) are considered in this application example. In the nonclassical damping case, the damping ratios obtained through complex modal analysis are (for modes 1 to 9): 5.31%, 2.09%, 9.47%, 3.62%, 2.39%, 12.22%, 3.95%, 2.47%, and 8.34%. The horizontal earthquake ground motion is imposed at 45° with respect to the X -axis.

Figures 13–15 show the EPSD functions of the displacement responses U_{X_3} (displacement relative to the ground of the third floor in the X -direction), U_{Y_3} (displacement relative to the ground of the third floor in the Y -direction), and θ_{Z_3} (rotation relative to the ground of the third floor about the vertical Z -axis), respectively, of the classically damped system to GMM I and GMM II fitted to the 1940 El Centro record. It is observed that the MDOF building system responses to GMM I and GMM II have similar modal contributions, namely: (i) $U_{X_3}(t)$ is almost exclusively determined by the first mode contribution (translation in the X -direction with $\omega_1=16.0$ rad/s); (ii) $U_{Y_3}(t)$ is almost

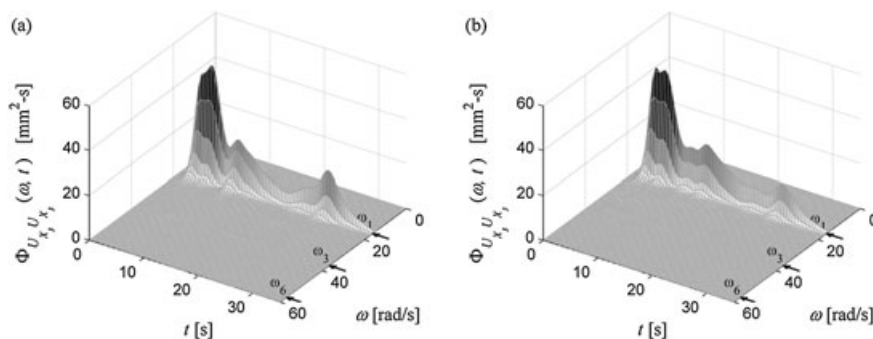


Figure 13. EPSD of U_{X_3} (classically damped building, El Centro 1940): (a) GMM I and (b) GMM II.

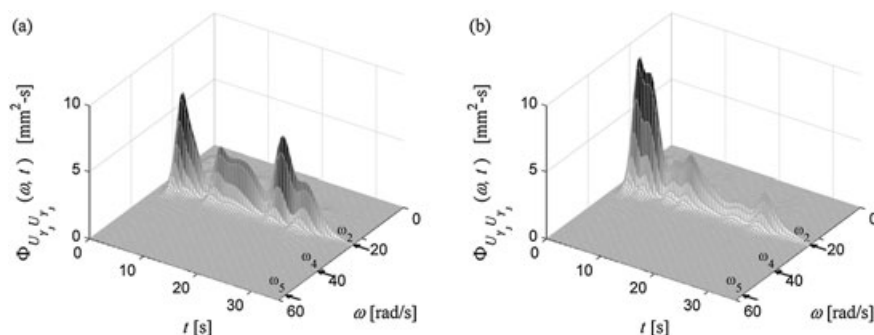


Figure 14. EPSD of U_{Y_3} (classically damped building, El Centro 1940): (a) GMM I and (b) GMM II.

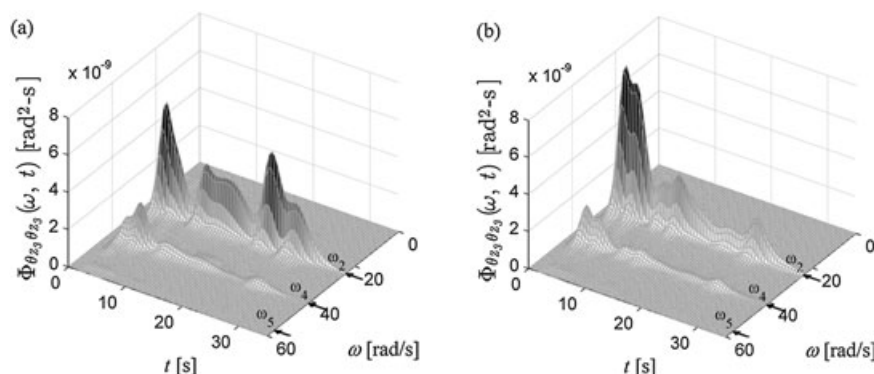


Figure 15. EPSD of θ_{Z_3} (classically damped building, El Centro 1940): (a) GMM I and (b) GMM II.

exclusively determined by the second mode contribution (lateral–torsional coupling in the Y -direction with $\omega_2=24.1$ rad/s); and (iii) $\theta_{Z_3}(t)$ not only is dominated by the second mode but also presents a significant contribution from the fourth mode (lateral–torsional coupling in the Y -direction with $\omega_4=41.2$ rad/s) and a very small but non-negligible contribution from the fifth mode (lateral–torsional coupling in the Y -direction with $\omega_5=56.7$ rad/s). However, significant differences are observed between the EPSDs of the stochastic responses $U_{Y_3}(t)$ and $\theta_{Z_3}(t)$ ($\Phi_{U_{Y_3}U_{Y_3}}(\omega, t)$ and $\Phi_{\theta_{Z_3}\theta_{Z_3}}(\omega, t)$, respectively) to GMM I and GMM II fitted to the El Centro 1940 record (Figures 14 and 15, respectively). On the other hand, the topology of the EPSD of $U_{X_3}(t)$, $\Phi_{U_{X_3}U_{X_3}}(\omega, t)$, is not significantly affected by the time-varying frequency content; that is, Figure 13(a) and 13(b) are not very different. Thus, the time-varying frequency content affects significantly only some of the stochastic response quantities for the building model considered here. Additional results for the Capitola 1989 and Orion Blvd. 1971 can be found in the study of Li *et al.* [22].

To illustrate the use of the new analytical solutions presented in this paper for evolutionary cross-PSD functions between ground motion input and structural response, given in Eqs. (34) and (51), Figure 16 shows the evolutionary cross-PSD functions, $\Phi_{\ddot{U}_g\theta_{Z_3}}(\omega, t)$, between the ground motion input $\ddot{U}_g(t)$ and the structural response $U_{\theta_3}(t)$ for GMM I and GMM II fitted to the El Centro 1940 record. Because the evolutionary cross-PSD function is complex valued, its real part (i.e., evolutionary cospectrum) and imaginary part (i.e., evolutionary quad-spectrum) are plotted separately. Unlike the EPSD of $\theta_{Z_3}(t)$, $\Phi_{\theta_{Z_3}\theta_{Z_3}}(\omega, t)$, the evolutionary cross-PSD function $\Phi_{\ddot{U}_g\theta_{Z_3}}(\omega, t)$, especially its real part, provides not only the temporal evolution of the energy of the structural response at the system natural frequencies but also the time-frequency distribution of the ground motion. Comparing Figure 16(a) and 16(b), it is observed that the evolutionary cospectrum of $\ddot{U}_g(t)$ and $\theta_{Z_3}(t)$ has a significant frequency content nonstationarity for GMM I, whereas the frequency content nonstationarity is lost for GMM II.

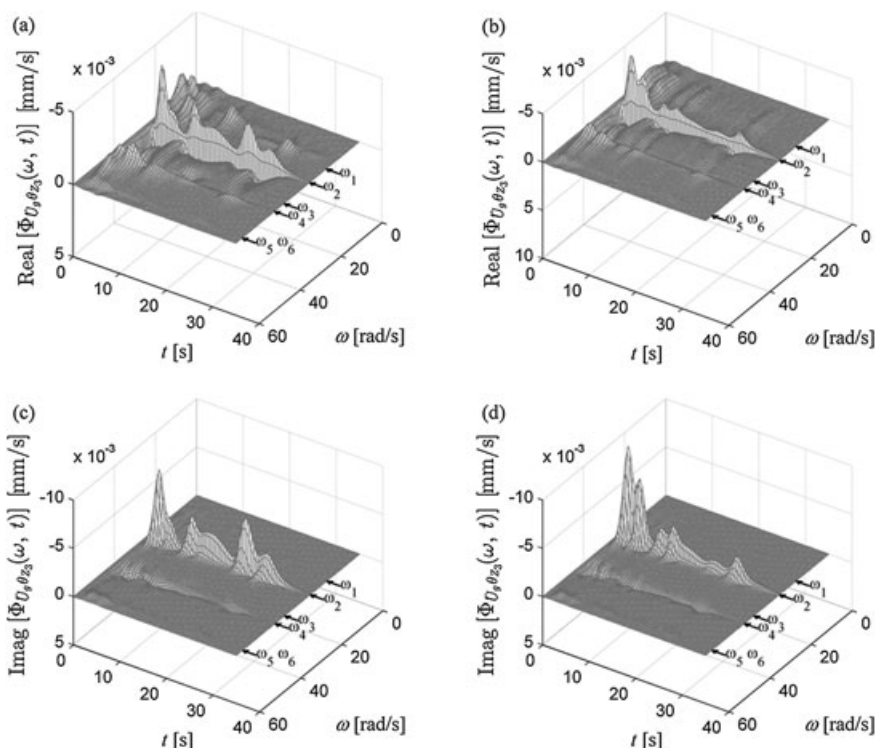


Figure 16. Evolutionary cross-PSD of \ddot{U}_g and θ_{z_3} under El Centro 1940: (a) real part for GMM I, (b) real part for GMM II, (c) imaginary part for GMM I, and (d) imaginary part for GMM II.

Figures 17–19 show the time histories of the RMS of the floor responses $U_{X_i}(t)$, $U_{Y_i}(t)$, and $\theta_{z_i}(t)$ (where $i = 1, 2, 3$ denotes the i -th floor) of the classically and nonclassically damped building models for GMM I and GMM II fitted to the El Centro 1940 record. The differences between GMM I and GMM II affect the RMS floor displacement and rotation responses to various degrees depending on the spectrotemporal properties of the target earthquake record. For example, in Figure 18(a), the difference between the RMSs of displacements at the third floor, $U_{Y_3}(t)$, of the classical-damped MDOF system subjected to GMM I and GMM II, respectively, is 13% at $t = 2.8$ s and 54% at $t = 22$ s, which is significant. In particular, for a given target earthquake record, the amplitude of the differences between the RMS responses to GMM I and GMM II depends on how significant the time variation of the seismic input’s frequency content is in the neighborhood of the natural frequencies associated with vibration modes contributing to the specific response quantity of interest. These differences in the RMS floor displacement and rotation responses expose the effects of time averaging the frequency content of GMM II compared with GMM I. Note that the dampers

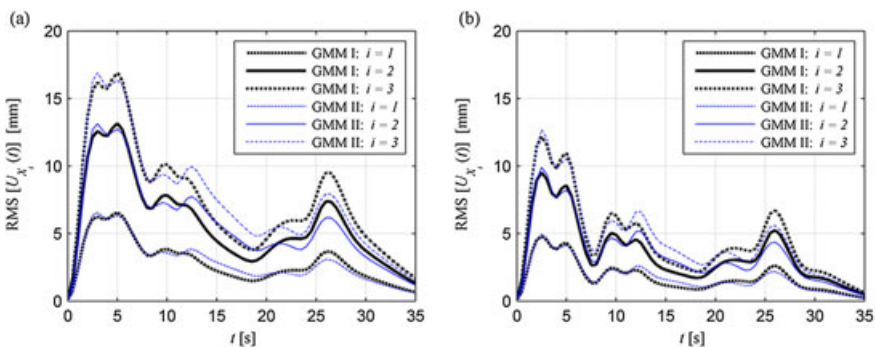


Figure 17. RMS of displacement responses $U_{X_i}(t)$ under El Centro 1940: (a) classically damped and (b) nonclassically damped.

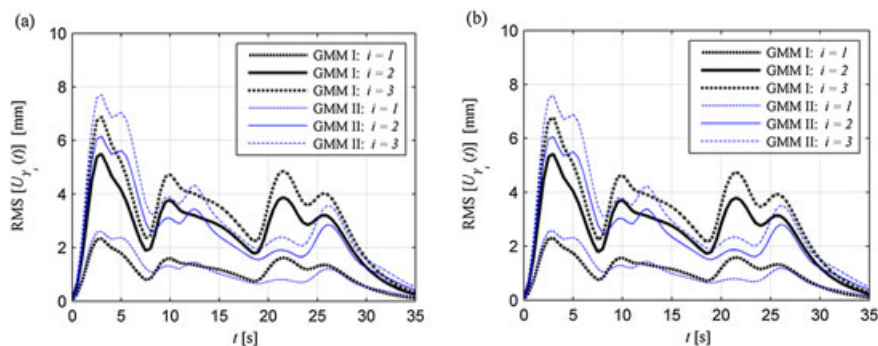


Figure 18. RMS of displacement responses $U_{Y_i}(t)$ under El Centro 1940: (a) classically damped and (b) nonclassically damped.

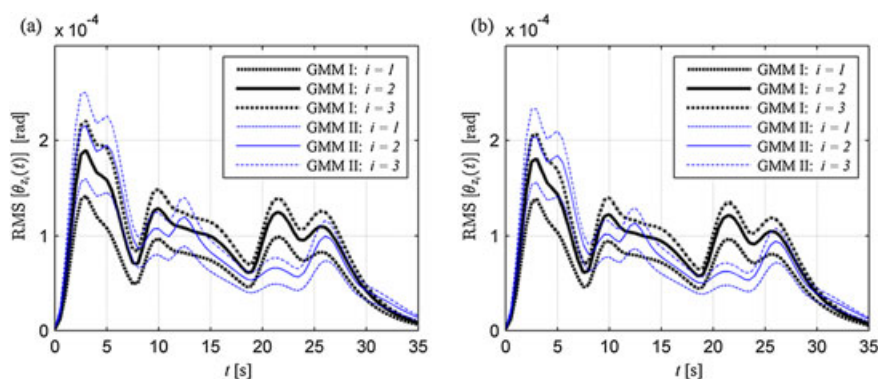


Figure 19. RMS of rotation responses $\theta_{Z_i}(t)$ under El Centro 1940: (a) classically damped and (b) nonclassically damped.

are placed in vertical planes along the X -direction and thus play a significant role in the structural response in the X -direction (Figure 17(a) and 17(b)), whereas they have little effects on the structural response in the Y -direction, as it can be observed by comparing Figure 18(a) and 18(b). Additional results for the Capitola 1989 and Orion Blvd. 1971 can be found in the study of Li *et al.* [22] and are qualitatively very similar to those presented here.

6. CONCLUSIONS

Two comparative and closely related stochastic earthquake ground motion models are used to investigate the effects of the temporal nonstationarity in the frequency content of earthquake ground motions on the response of linear elastic models of structural systems. A new stochastic ground motion model (GMM II), nonstationary in amplitude only, is derived from a previously developed fully nonstationary (i.e., nonstationary in both amplitude and frequency content) stochastic earthquake ground motion model (GMM I) fitted to a target earthquake ground acceleration record. Both stochastic ground motion models have the same mean-square function and globally time-averaged PSD function (frequency content). Explicit closed-form solutions for the stochastic response of linear elastic SDOF and MDOF systems subjected to GMM II are derived, in addition to new solutions for the evolutionary cross-correlation and cross-PSD functions between the seismic input and the structural response for GMM I. The closed-form solutions are presented and applied to linear elastic SDOF and MDOF systems subjected to the two ground motion models fitted to target real earthquake records. This paper compares the spectrotemporal stochastic properties of system response quantities, including the evolutionary auto/cross-correlation and auto/cross-power spectral

densities of system responses, evolutionary cross-correlation and cross-power spectral densities between earthquake input and system response, and RMS system response. Through this comparison, more insight is gained into the effects of the spectral nonstationarity of the seismic input on the system response. It is observed that the time-varying frequency content in the seismic input may have a significant effect on the stochastic properties of the system response, depending on the time-frequency distribution of the seismic record and the dynamic properties of the system. Therefore, for rational and reliable earthquake-resistant design and analysis, it is necessary to use a fully nonstationary earthquake ground motion model, which captures the temporal nonstationarity in the frequency content. The analytical random vibration solutions presented in this paper can be used to evaluate, using analytical approximations, the first-passage probability of the response of linear dynamic systems [24] or, in other words, the statistics of the peak structural response, which are of significant practical interest. These solutions can also be readily used in equivalent linearization methods of nonlinear stochastic dynamics such as the tail-equivalent linearization method for nonlinear random vibration [25]. Finally, they provide benchmark exact solutions to validate, in the linear range of structural behavior, numerical methods of stochastic dynamics developed for linear and nonlinear systems.

The pair of comparative and closely related stochastic earthquake ground motion models presented herein can be further used to investigate the effect of the time-varying frequency content of actual earthquake ground motions on the response of nonlinear elastic and inelastic structural systems, for example, moving resonance effects. The extension of the study presented here for nonlinear systems using the Monte Carlo simulation approach (i.e., performing statistical analysis of ensemble time history analyses using artificial ground motions simulated from GMM I and GMM II) is the subject of ongoing research.

ACKNOWLEDGEMENTS

Partial support of this research by the Pacific Earthquake Engineering Research Center's Transportation Systems Research Program under award no. 1107-NCTRCJ, with Prof. Steve Mahin as the Pacific Earthquake Engineering Research director, and the Louisiana Department of Wildlife and Fisheries through award no. 724534, is gratefully acknowledged. Any opinions, findings, conclusions, or recommendations expressed in this publication are those of the authors and do not necessarily reflect the views of the sponsors.

REFERENCES

1. Yamamoto Y, Baker JW. Stochastic model for earthquake ground motion using wavelet packets. *Bulletin of the Seismological Society of America* 2013; **103**(6):3044–3056.
2. Huang D, Wang G. Stochastic simulation of regionalized ground motions using wavelet packets and cokriging analysis. *Earthquake Engineering & Structural Dynamics* 2015; **44**:775–794. DOI:10.1002/eqe.2487.
3. Der Kiureghian A, Crempien J. An evolutionary model for earthquake ground motion. *Structural Safety* 1989; **6**(2-4):235–246. DOI:10.1016/0167-4730(89)90024-6.
4. Conte JP, Peng B-F. Fully nonstationary analytical earthquake ground motion model. *Journal of Engineering Mechanics* 1997; **123**(1):15–24.
5. Rezaeian S, Der Kiureghian A. Simulation of synthetic ground motions for specified earthquake and site characteristics. *Earthquake Engineering & Structural Dynamics* 2010; **39**:1155–1180. DOI:10.1002/eqe.997.
6. Deodatis G, Shinozuka M, Papageorgiou A. Stochastic wave representation of seismic wave representation of seismic ground motion. II: simulation. *Journal of Engineering Mechanics* 1990; **116**(11):2381–2399. DOI:10.1061/(ASCE)0733-9399(1990)116:11(2381).
7. Zhang R, Yong Y, Lin YK. Earthquake ground motion modeling. II: stochastic line source. *Journal of Engineering Mechanics* 1991; **117**(9):2133–2148.
8. Lin YK, Yong Y. Evolutionary Kanai-Tajimi earthquake models. *Journal of Engineering Mechanics* 1987; **113**(8):1119–1137. DOI:10.1061/(ASCE)0733-9399(1987)113:8(1119).
9. Beck JL, Papadimitriou C. Moving resonance in nonlinear response to fully nonstationary stochastic ground motion. *Probabilistic Engineering Mechanics* 1993; **8**(3–4):157–167.
10. Boore DM. Simulation of ground motion using the stochastic method. *Pure and Applied Geophysics* 2003; **160**(3-4):635–676.
11. Saragoni GR, Hart GC. Nonstationary analysis and simulation of earthquake ground motions. *Report No. UCLA-ENG-7238*, Earthquake Engineering and Structures Laboratory, University of California at Los Angeles, CA, 1972.
12. Grigoriu M, Ruiz SE, Rosenblueth E. The Mexico earthquake of September 19, 1985 – nonstationary models of seismic ground acceleration. *Earthquake Spectra* 1988; **4**(3):551–568. DOI:10.1193/1.1585490.

13. Yeh CH, Wen YK. Modeling of nonstationary ground motion and analysis of inelastic structural response. *Structural Safety* 1990; **8**(1-4):281–298. DOI:10.1016/0167-4730(90)90046-R.
14. Brune JN. Tectonic stress and the spectra of seismic shear waves from earthquakes. *Journal of Geophysical Research* 1970; **75**:4997–5009.
15. Conte JP. Effects of earthquake frequency nonstationarity on inelastic structural response. *Proc. 10th World Conference on Earthquake Engineering*, Spain, 1992; 3645–3651.
16. Conte JP, Pister KS, Mahin SA. Nonstationary ARMA modeling of seismic motions. *Soil Dynamics and Earthquake Engineering* 1992; **11**(7):411–426. DOI:10.1016/0267-7261(92)90005.
17. Naga P, Eatherton MR. Analyzing the effect of moving resonance on seismic response of structures using wavelet transforms. *Earthquake Engineering & Structural Dynamics* 2013; **43**(5):759–768.
18. Wang L, McCullough M, Kareem A. Modeling and simulation of nonstationary processes utilizing wavelet and Hilbert transforms. *Journal of Engineering Mechanics* 2014; **140**:345–360.
19. Wang J, Fan L, Qian S, Zhou J. Simulations of non-stationary frequency content and its importance to seismic assessment of structures. *Earthquake Engineering & Structural Dynamics* 2002; **31**(4):993–1005. DOI:10.1002/eqe.134.
20. Peng B-F, Conte JP. Closed-form solutions for the response of linear systems to fully nonstationary earthquake excitation. *Journal of Engineering Mechanics* 1998; **124**(6):684–694.
21. Priestley MB. *Spectral Analysis and Time Series*. Academic Press: New York, N.Y., 1987.
22. Li Y, Conte JP, Barbato M. Closed-form solutions for the stochastic response of linear elastic systems to earthquake ground motion models with and without frequency nonstationarity. *Report No. SSRP-15/04*, University of California, San Diego, 2015.
23. Lin YK. *Probabilistic Theory of Structural Dynamics*. Krieger Publishing Co.: Melbourne, FL., 1976.
24. Barbato M, Conte JP. Time-variant reliability analysis of linear elastic systems subjected to fully nonstationary stochastic excitations. *Journal of Engineering Mechanics* 2014; **141**(6). DOI:10.1061/(ASCE)EM.1943-7889.0000895, 04014173.
25. Fujimura K, Der Kiureghian A. Tail-equivalent linearization method for nonlinear random vibration. *Probabilistic Engineering Mechanics* 2007; **22**:63–76.